Supplementary information - Elastic instabilities during flow of hydrolyzed poly-acrylamide solution in porous media: Effect of pore-shape and salt

Durgesh Kawale[a,b,c], Esteban Marques[b] Pacelli L. J. Zitha[a], Michiel T. Kreutzer[b], W. R. Rossen[a], and Pouyan E. Boukany[b*]

[a]Department of Geosciences and Engineering, Delft University of Technology, Stevinweg 1, Delft, The Netherlands;

[b]Department of Chemical Engineering, Delft University of Technology, Julianalaan 136, Delft, The Netherlands;

[c]Dutch Polymer Institute (DPI), P.O. Box 902, 9600 AX, Eindhoven, The Netherlands.

[*] E-mail: P.E.Boukany@tudelft.nl

---

1. One movie (SM-1) is included in the supplementary information, showing the different flow regimes in the square, staggered geometry. The movie contains streamlines at three different shear rates for 0.1 % HPAM solution (without salt) (i) $\dot{\gamma}_{\text{app}} = 3.63\,\text{s}^{-1}$ ($Wi = 78.2$, $Re = 8 \times 10^{-4}$), (ii) $\dot{\gamma}_{\text{app}} = 29.07\,\text{s}^{-1}$ ($Wi = 626.5$, $Re = 1.6 \times 10^{-2}$), and (iii) $\dot{\gamma}_{\text{app}} = 145.33\,\text{s}^{-1}$ ($Wi = 3131$, $Re = 2.5 \times 10^{-1}$)

2. Table S1 shows the shear rheology fit results to the Carreau-Yasuda model for all the HPAM solutions used in the current study.

3. Fig S1 shows the small amplitude oscillatory strain measurements of all the HPAM solutions used in the current study.

4. Comparison between global shear rate calculation and local shear rate calculation was performed using PIV for a circle, staggered geometry having diameter of 195 µm and height of 85 µm. From PIV, the calculated shear rate was $5.22\,\text{s}^{-1}$, whereas the global shear rate calculation yields $4.6\,\text{s}^{-1}$. In fig. S2 we show these results.

5. Fig S3 shows mechanical degradation of 0.2 % HPAM solution with 17 mmol NaCl. This solution relaxation time is $\sim$3 s, and our test shows that the shear viscosity of fresh solution is same as a solution that was pre-sheared for 120 s at $500\,\text{s}^{-1}$ in a Couette geometry. There is no visible decrease in the shear viscosity for both these solution showing that this HPAM solution does not degrade upto shear rate of $500\,\text{s}^{-1}$ (or upto $Wi \sim 1500$).

6. Fig. S4 shows stable creeping flow of polymer solutions through the square, staggered geometry at $\dot{\gamma}_{\text{app}} = 0.007\,\text{s}^{-1}$ ($Wi = 0.1$).

7. Fig. S5 shows unprocessed ΔP measurements in the square staggered geometry for the flow of 0.1 % HPAM in DI water (no salt) at $\dot{\gamma}_{\text{app}} = 3.63\,\text{s}^{-1}$ and at $\dot{\gamma}_{\text{app}} = 145.33\,\text{s}^{-1}$.

8. Fig S6 shows dead zone washing steps at $\dot{\gamma}_{\text{app}} = 29.07\,\text{s}^{-1}$ for 0.1 % HPAM solution (without salt)

Table S1: Fit results from Carreau-Yasuda model

Polymer & NaCl concentration	η_0 (Pa s)	η_∞ (Pa s)	n (-)	τ (s)	a (-)
0.1 % HPAM, 0 mmol NaCl	6.65	0.001	0.28	21.55	0.62
0.2 % HPAM, 17 mmol NaCl	0.72	0.001	0.42	3.03	1.11
0.2 % HPAM, 170 mmol NaCl	0.08	0.001	0.61	0.76	0.88
0.2 % HPAM, 340 mmol NaCl	0.03	0.001	0.71	0.35	1.8
0.2 % HPAM, 680 mmol NaCl	0.02	0.001	0.72	0.17	1.30

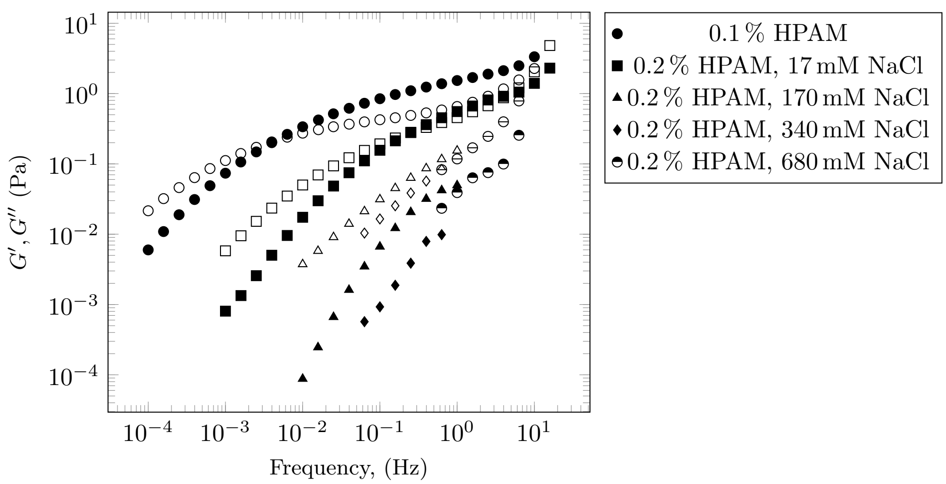

Figure S1: Small amplitude oscillatory strain measurements of all HPAM solutions used in the current study.

9. Fig S7 shows the power spectral density curves for flow of 0.1 % HPAM solution (without salt) in all the four geometries. In fig S8 power spectral density curves for all geometries at same apparent shear rate are plotted together, showing the the general shape of curve is same in all the geometries.

10. Fig S9 compares power spectral density of point-pressure fluctuations at the inlet pressure sensor (P_{inlet}) with that of the pressure drop fluctuations. The shape of the spectral density curves is same. Results for 0.2 % HPAM solution in 680 mmol NaCl flowing through the square staggered geometry at apparent shear rate of 60 s^{-1}.

11. Fig. S10 shows that the onset of apparent shear-thickening region for 0.2 % HPAM solution with 680 mmol NaCl starts with the elastic flow instabilities, which in turn is also marked by increase in the std(ΔP) fluctuations.

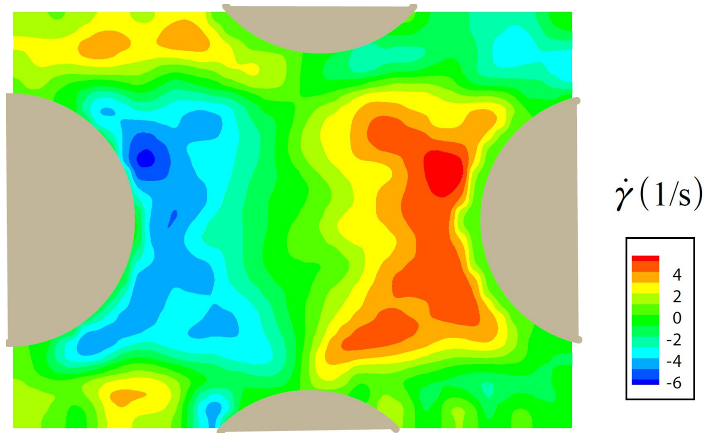

Figure S2: Local shear rate map for 0.1 % HPAM in DI water flowing through a circle, staggered geometry with volumetric flow of $Q = 4\,\mu\mathrm{L\,min^{-1}}$. The circle diameter is 195 µm, height of microfluidic device is 85 µm, porosity is 0.7. Flow direction is left to right. $\dot{\gamma}_{\mathrm{app}}^{PIV} = 5.22\,\mathrm{s^{-1}}$ and $\dot{\gamma}_{\mathrm{app}}^{global} = 4.6\,\mathrm{s^{-1}}$.

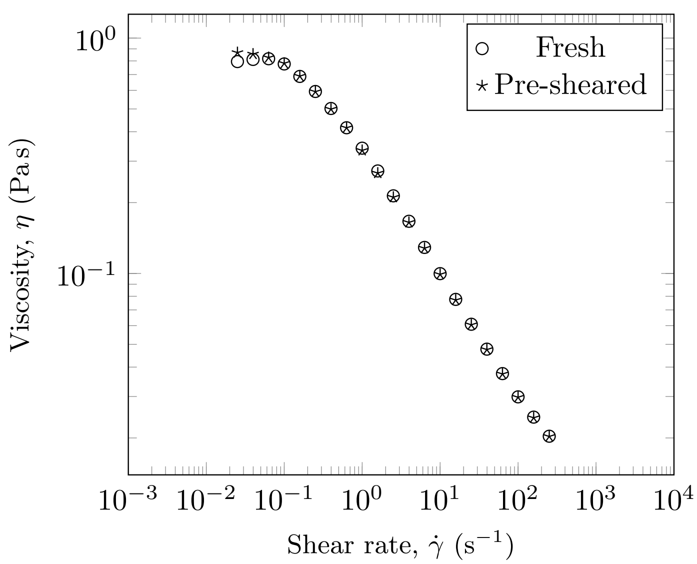

Figure S3: Mechanical degradation test for 0.2 % HPAM, 17 mmol NaCl solution. Pre-shear solution was sheared at $500\,\mathrm{s^{-1}}$ for 120 s. Measurement performed in a Couette geometry at $T = 22\,^{\circ}\mathrm{C}$.

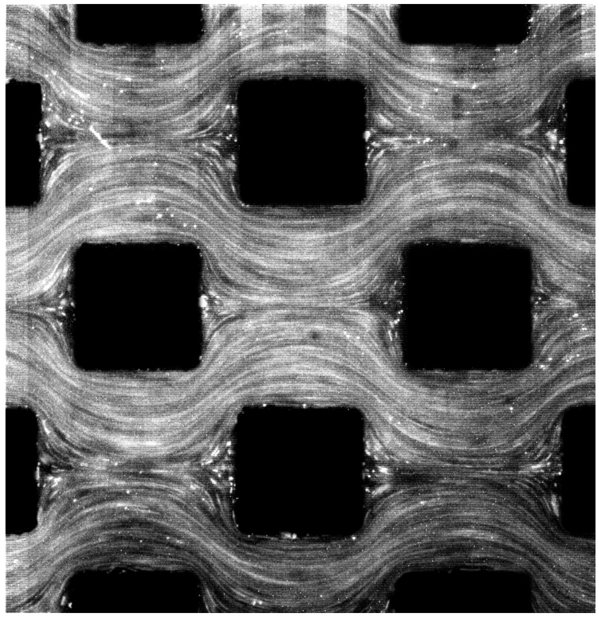

Figure S4: Streamlines showing creeping flow of polymer solutions in the square staggered geometry at $Wi = 0.1$. Flow direction is from left to right. Side of the square is 262 µm

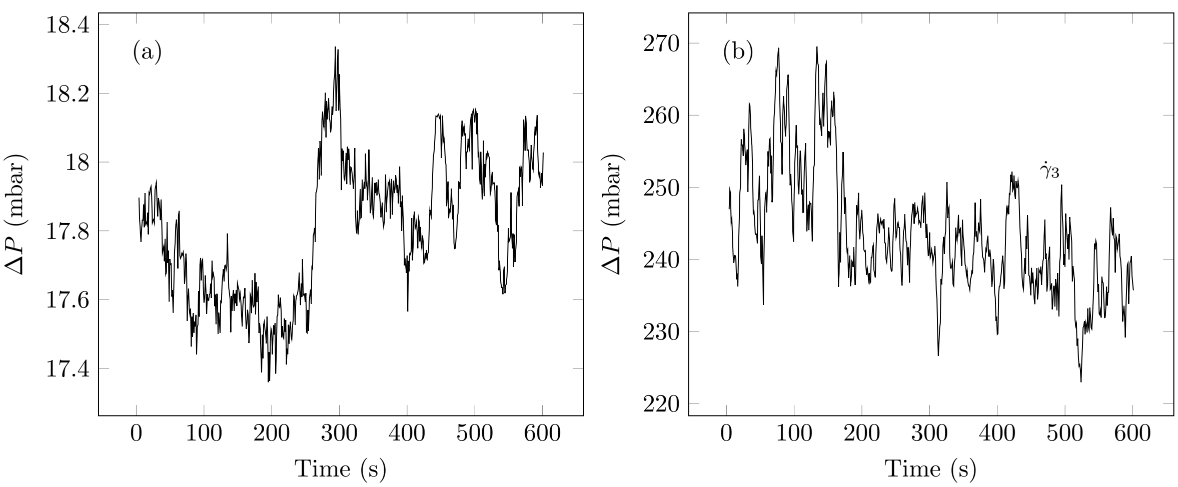

Figure S5: ΔP measurements in the square staggered for flow of 0.1 % HPAM in DI water (no salt). (a) $\dot{\gamma}_{app} = 3.63\,\mathrm{s}^{-1}$, (b) $\dot{\gamma}_{app} = 145.33\,\mathrm{s}^{-1}$.

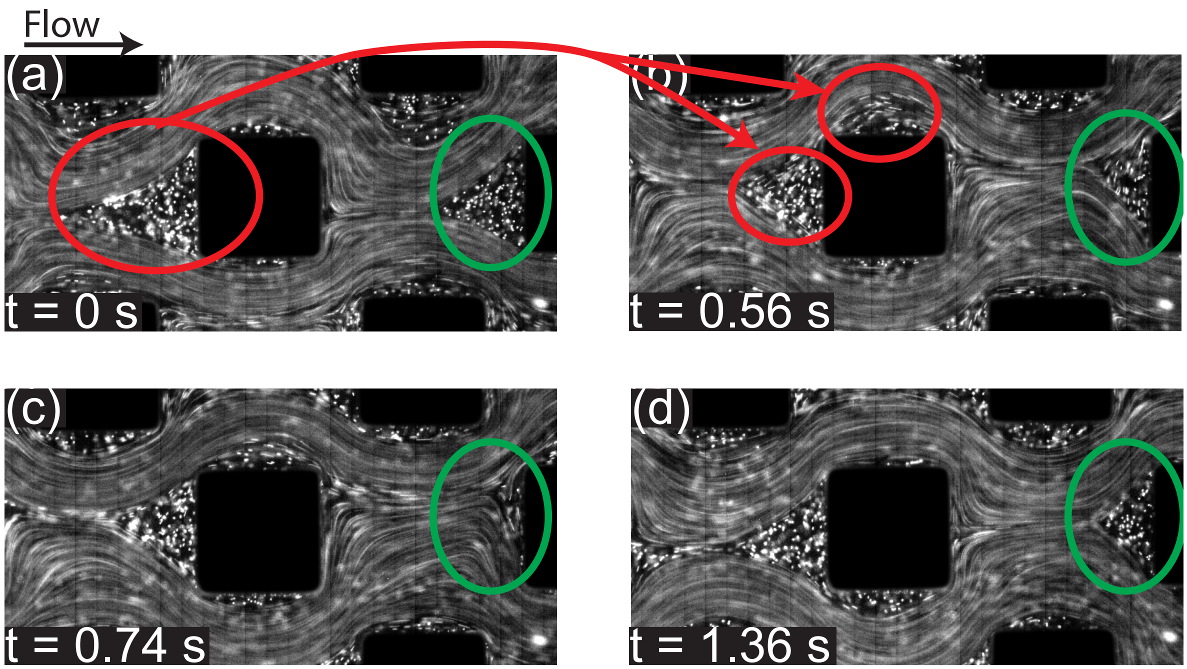

Figure S6: Dead zone washing can occur in one or two steps. In the single-step washing process, the complete dead zone is washed away. However, in the two-step process, it can wash a part of its mass, such that the (usually smaller) downstream dead zone can shed completely. (a) A fully grown dead zone wobbles perpendicular to the flow direction. (b) A part of the dead zone's mass (in red) is shed causing the downstream dead zone to start shedding (in green) and it rapidly sheds entirely. Notice the time stamps from (a) to (b) and then to (c). In (d) the vortex has grown to roughly half it's full-grown size, for which it took $1.36 - 0.74 = 0.62\,\mathrm{s}$.

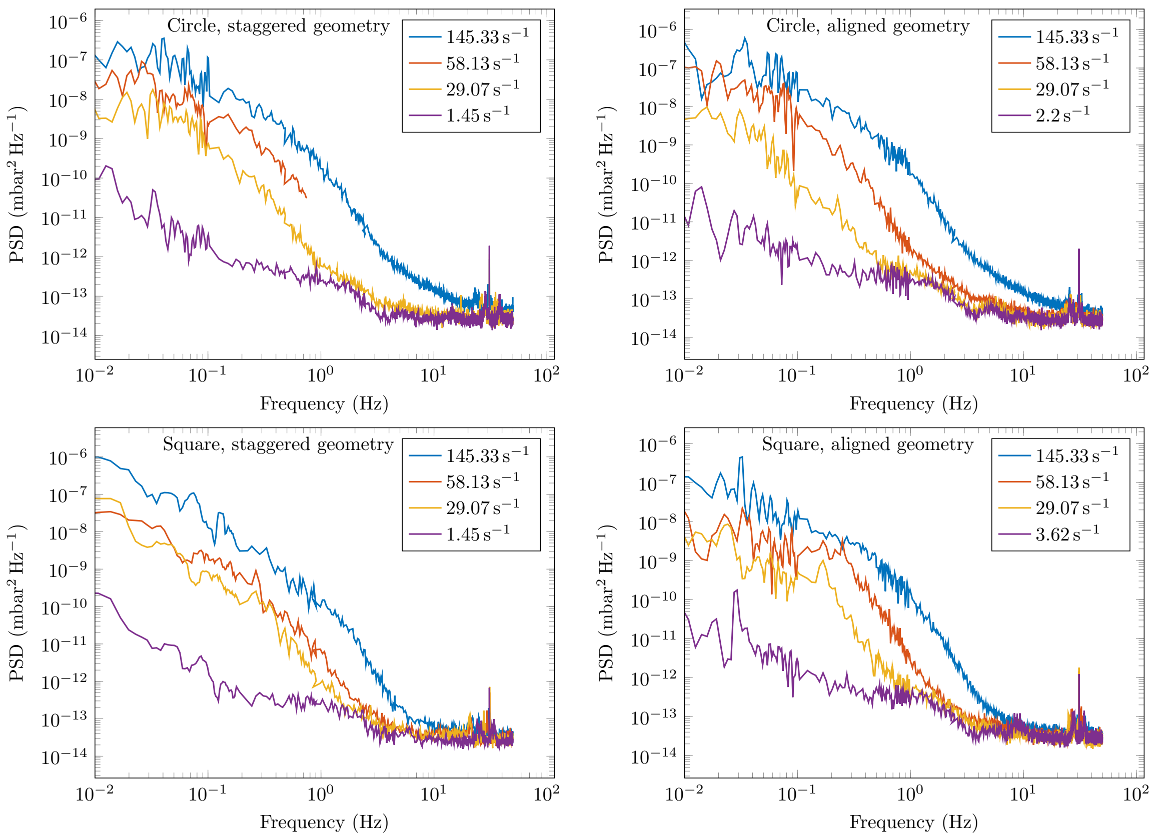

Figure S7: Power spectral density at various apparent shear rates for 0.1 % HPAM solution (without salt) flowing through all the four geometries.

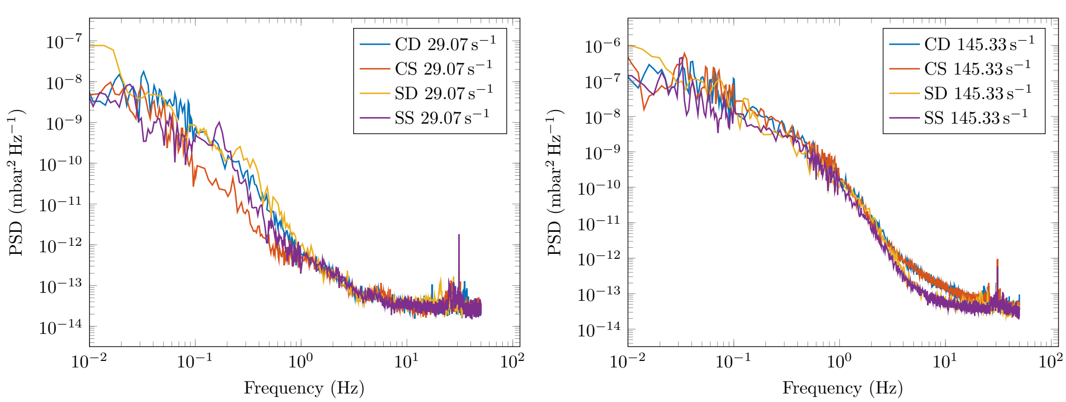

Figure S8: Left: Power spectral density curves at $\dot{\gamma}_{\text{onset}} = 29.07\,\text{s}^{-1}$ for all geometries. Right: Power spectral density curves at $\dot{\gamma}_{\text{app}} = 145.33\,\text{s}^{-1}$ for all geometries. CD = circle staggered, CS = circle aligned, SD = square staggered, SS = square aligned.

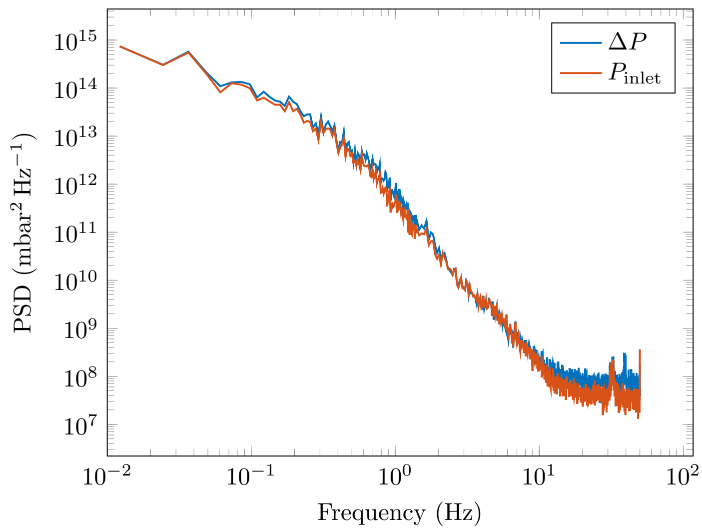

Figure S9: Power spectral density of ΔP fluctuations and P_{inlet} fluctuations for 0.2 % HPAM in 680 mmol NACl, $\dot{\gamma}_{\mathrm{app}} = 60\,\mathrm{s}^{-1}$.

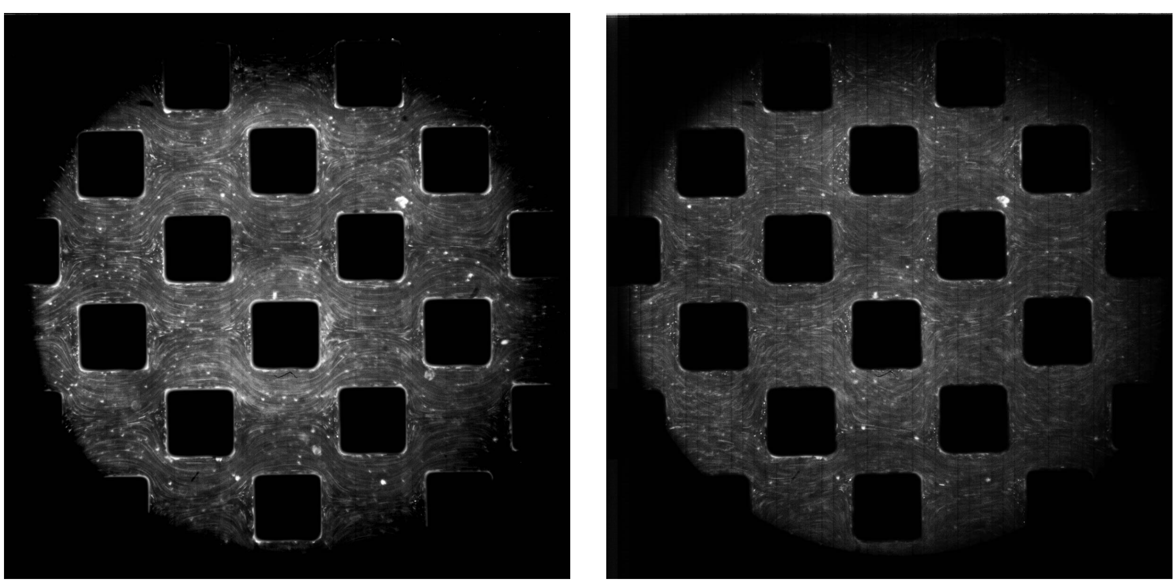

Figure S10: Streamlines showing that the elastic flow instabilities in HPAM solution with 680 mmol NaCl start at the onset shear rate for apparent shear-thickening region. Streamline snapshots at $\dot{\gamma}_{\mathrm{app}} = 15\,\mathrm{s}^{-1}$ (left) and $\dot{\gamma}_{\mathrm{app}} = 37.7\,\mathrm{s}^{-1}$ (right). Flow direction is left to right.